Phases of attractive two-dimensional vesicles under pressure

David H. Boal
Department of Physics, Simon Fraser University, Burnaby, British Columbia, Canada V5A 1S6
(Received 20 September 1990)

The phase diagram of a tethered-ring model for vesicles in two dimensions is investigated. Each element on the vesicle's perimeter is subject to attraction to other elements, and the vesicle as a whole is under pressure. Four different phases, characterized by their scaling exponents, are found to be present in this range of parameter space: inflated, dense, self-avoiding-walk, and branched phases. An approximate phase diagram at small pressure is determined.

I. INTRODUCTION

Many characteristics of polymers, membranes, and vesicles have been determined by computer-simulation techniques.[1] The computational study of vesicles at finite temperatures has generally been limited to two dimensions because of the long relaxation times associated with large vesicles embedded in three dimensions. Currently, computer models of three-dimensional vesicles[2–4] are necessarily coarse grained and are most appropriate for studying gross structural properties. Two-dimensional vesicles have been modeled as closed polymer chains subject to a pressure difference across the chain. Studies[5,6] of such chains show that their scaling characteristics (size as a function of mass) vary with pressure and with bending rigidity along the chain.

In particular, it is shown in Refs. 5 and 6 that at zero bending rigidity, vesicle-size scaling behavior changes from that of a self-avoiding walk at zero pressure difference, to either a branched polymer at negative pressure, or an inflated ring at positive pressure. The sign convention we adopt is that the pressure difference is positive if the internal pressure exceeds the external pressure. Duplantier points out[7] that the branched-polymer phase at zero rigidity should be different from the dense phase expected if the elements of the vesicle's perimeter were attractive.

In this paper, we investigate the domains of these phases—inflated, dense, self-avoiding walk (SAW), and branched phases—for attractive vesicles under pressure. In Sec. II, we outline our vesicle model and the computational techniques used in the simulation. In Sec. III we extract the phase dependence of the scaling behavior and of the energetics of the vesicles. Our results are discussed and summarized in the conclusion.

II. COMPUTATIONAL TECHNIQUE

The calculational technique we use is the traditional Metropolis Monte Carlo method at fixed pressure and temperature.[8] Monte Carlo simulations of membranes in three dimensions have often been based on the tethered-membrane model of Kantor, Kardar, and Nelson.[9] The model represents the membrane as a triangulated network of beads attached by flexible strings or tethers. With bending rigidity, the tethered membrane possesses a transition from a low-temperature flat phase to a high-temperature crumpled phase if long-rang self-avoidance is omitted.[9] For truly self-avoiding membranes, the phase transition is absent.[10] In the limited studies of three-dimensional vesicles performed so far,[2] it is found that scaling behavior may also depend on the connectivity of the membrane.

Leibler, Singh, and Fisher[5] use the tethered-membrane approach as a model for vesicles in two dimensions. The boundary of the vesicle is represented by a ring of beads each of diameter a. The tethering constraint is enforced through the use of a step-function potential that is infinitely repulsive at bead center-to-center distances less than a (for all bead pairs) or greater than $2a$ (for nearest-neighbor pairs). The first constraint implies that there is a minimum perimeter for a given number of beads N. The second constraint assures self-avoidance of the ring in the limit of small bead movement. In actual practice, the maximum allowable nearest-neighbor bead separation must be made slightly less than $2a$ in order to prevent a bead from "stepping across" a remote part of the ring in a single finite Monte Carlo trial move.

Our model potential energy V includes not only the step-function potentials enforcing self-avoidance and tethering, but also an attractive term between all beads on the ring:

$$\beta V = -\beta k_a \sum_{i<j} r_{ij}^{-6} + S \ , \tag{1}$$

where r_{ij} is the separation between beads i and j, S represents the step functions, and β is the inverse temperature. For convenience, we rewrite the attraction parameter k_a as $\kappa_a = \beta k_a / a^6$ and refer to κ_a as the attraction. The vesicles are also subject to a pressure difference $\Delta p = p_{\rm int} - p_{\rm ext}$ across the ring. In the simulations, we refer to $\Pi = \beta a^2 \, \Delta p$ as the pressure. With this sign convention for Δp, the enthalpy H of the system is then

$$\beta H = \beta E - \Pi A \ , \tag{2}$$

where E is the expectation of the potential energy of Eq. (1) and A is the enclosed area of the vesicle in units of a^2. The bead momenta are omitted in this simulation, since they are not required for the observables of interest.

In the Monte Carlo procedure we use, a trial position for a member of the ring is chosen randomly from within a coordinate space box of fixed size (a square of length $2s$ to the side) centered on the bead's current position. We choose to move beads in pairs, so that the algorithms can be used for fixed-area simulations,[11] as well as the fixed-pressure results reported here. A sweep around the ring consists of making a trial move on each bead i in sequence 1 to N. For each bead i, a mate j is randomly chosen from any site on the ring (except the nearest-neighbor sites) and trial positions are selected for i and j simultaneously. Hence, one sweep around the ring involves trial moves on $2N$ particles. The trial move is accepted conditionally depending on the enthalpy change associated with it. With the step size $s=0.1$, 20–80% of the particles are moved per sweep, depending on the temperature.

Our Monte Carlo algorithm produces successive configurations that are highly correlated, and it is important to determine the "time" scale on which such correlations decay. We define an autocorrelation function for an observable O by

$$C(\Delta t)=\langle [O(t+\Delta t)-\langle O\rangle][O(t)-\langle O\rangle]\rangle/\langle [O(t)-\langle O\rangle]^2\rangle , \tag{3}$$

where the angular brackets indicate an average over Monte Carlo steps labeled by the time variable t. Numerically, we observe the correlation function for the vesicle's moments of inertia to decay roughly exponentially with time. For the zero-pressure and zero-attraction case, the time constants of the decay are in the range of 10 000–20 000 sweeps around the ring for $s=0.1$ and $N=64$, the time constant depending on the temperature. Based on this value and its dependence on N and s, we empirically define a relaxation time τ of

$$\tau\equiv(N/4s)^2 . \tag{4}$$

This dependence of τ on ring width is found to be similar to the Rouse relaxation time.[12] For each parameter combination discussed below, an initially circular configuration is propagated for 200τ (at zero pressure) or 100τ (at finite pressure) with a sample configuration being stored every τ sweeps around the ring. The first ten configurations are omitted from the analysis, since the circular-ring initialization may not be similar to the "average" configuration for some Π-κ_a combinations. For the largest ring sizes considered, $N=192$, at least 4×10^7 trial moves are made per bead for each parameter set in the simulations. Computer limitations have restricted us to ring sizes in the range $64\le N\le192$ since the execution time of the code increases faster than N^3. This range of N is sufficient to allow the investigation of some, but not all, finite-size effects. The largest rings required 200–400 CPU hours per parameter set to execute on an MIPS R3000 processor. The entire data set required more than a CPU year to generate.

III. RESULTS

The vesicles in a given part of Π-κ_a parameter space can be characterized by how their rms radius and area scale with mass:

$$\langle r^2\rangle \propto N^{2\nu} , \tag{5a}$$

$$\langle A\rangle \propto N^{2\eta} . \tag{5b}$$

Within the uncertainty of their simulation, Leibler, Singh, and Fisher[5] find that $\nu=\eta=3/4$ for $\Pi=\kappa_a=0$. For a self-avoiding random walk in two dimensions, it has been shown[13] that $\nu=\frac{3}{4}$ and also established[7] that $\nu=\eta$. For $\Pi<0$, $\kappa_a=0$, the vesicle shapes are observed[5] to be consistent with those of a branched polymer,[14] $\nu=0.64$ and $\eta=0.5$. For positive pressures $\Pi>0$ and $\kappa_a=0$, they find $\nu=1$–1.5, which is consistent with inflated vesicles.

What do we expect to find in the $\kappa_a>0$ region? Let us consider three situations.

(a) $\Pi=0$. Here, the system should possess a Θ point like a simple polymer chain.[15] For small κ_a, the vesicle should behave like a self-avoiding random walk with $\nu=\eta=\frac{3}{4}$, while for large κ_a, the vesicle should become dense with $\nu=\eta=\frac{1}{2}$.

(b) $\Pi<0$. For $\Pi<0$, there should be a branched-polymer phase at small κ_a. This region is distinct from the dense phase expected at large κ_a and $\Pi=0$ or $\Pi<0$.

(c) $\Pi>0$. Because of its short-range nature, the attractive term will contribute a maximum of about $(-)3\kappa_a$ per particle to the energy even when the beads are close packed. Therefore, the attractive energy grows no faster than N as the ring size increases. The area of SAW vesicles grows like $N^{3/2}$, while that of inflated vesicles grows like N^2, so that for $\Pi>0$, the pressure contribution ultimately dominates the attractive piece at large N. Hence, we expect that the vesicles will always be inflated for $\Pi>0$, although finite-size effects are nontrivial, as is shown below.

A summary of the expected behavior is shown in Fig. 1, in which the dense phase includes the $\Pi=0$ axis. The different phases are assumed to have a "quadruple point" at $\Pi=0$ and intermediate κ_a. In fact, de Gennes[16] has shown that the polymer Θ point is a tricritical point.[17] Scaling in the tricritical region is more complicated than the simple forms of Eqs. (5). Hence, our ability to determine the order of the transition in the tricritical region is limited, as we discuss below.

Armed with some intuition about vesicle behavior in Π-κ_a parameter space, we turn now to the simulation results. The simulations are run at three different pressures, $\Pi=0.1$, 0, and -0.1. To graphically illustrate the shapes of the vesicles in the different phases, we show in Fig. 2 configurations taken from the $N=192$ simulations. The top and bottom rows of the figure correspond to $\Pi=0$ and -0.1, respectively, while the left and right columns correspond to $\kappa_a=1.5$ and 2.5, respectively. All of the configuration are drawn to the same scale. Vesicles

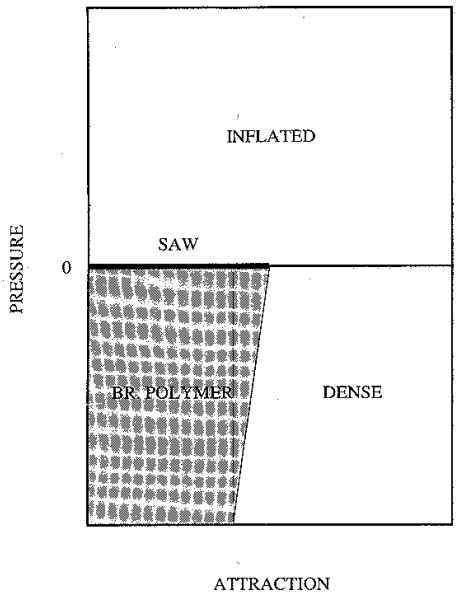

FIG. 1. Schematic phase diagram for model vesicles as a function of pressure (Π) and attraction (κ_a). The dense phase includes the $\Pi=0$ axis.

at $\Pi=0.1$ are inflated and are so large in area that they are omitted from the figure so as to show more clearly the behavior of the other phases. Configurations (b) and (d) are in the dense phase with $\nu=\frac{1}{2}$. Configuration (a) is in the SAW phase, while (c) is in the branched-polymer phase. The shape characteristics of each of these phases are clearly visible in Fig. 2.

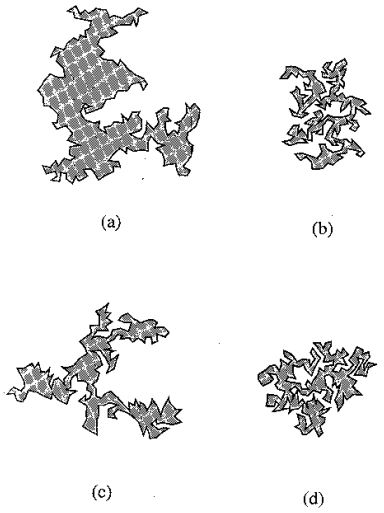

FIG. 2. Representative samples of 192-element vesicles shown for several parameter choices. The top [(a) and (b)] and bottom [(c) and (d)] rows have $\Pi=0$ and -0.1, respectively, while the left [(a) and (c)] and right [(b) and (d)] columns have $\kappa_a=1.5$ and 2.5, respectively. All configurations are drawn to the same scale.

The transition from the SAW phase to the dense phase at $\Pi=0$ is shown in Fig. 3, in which both scaling exponents ν and η are shown as a function of κ_a. First, one can see that within our estimated exponent error of ±0.03, ν and η are equal over the κ_a range investigated. They both change at around $\kappa_a=2\pm0.2$ from the SAW value of $\nu=\eta=\frac{3}{4}$ to the dense value of $\nu=\eta=\frac{1}{2}$. To define the transition point to better accuracy we would have to run the simulation for finer steps in κ_a than 0.25 and for much larger N, since finite-size and other corrections are important in this region.[16–21]

The transition from the branched-polymer phase to the dense phase is shown in Fig. 4 for the same scaling exponents ν and η as shown in Fig. 3. One can see that the radius exponent ν changes from the branched-polymer value of 0.64 to the dense-phase value of $\frac{1}{2}$ at around $\kappa_a=2$. The value of η is equal to $\frac{1}{2}$ for both the branched-polymer and dense phases, and this behavior is found in the figure. We are unable to determine whether this transition occurs at a larger or smaller value of κ_a than does the SAW phase to dense-phase transition at $\Pi=0$.

For $\Pi>0$ there is competition between the pressure and attractive terms in which finite-size effects play a role. Let us consider two extreme situations. If the attraction is very strong compared to the pressure, then the system is nearly close packed with each bead having roughly six nearest neighbors in the large-N limit. The corresponding enclosed area is roughly $N\pi(a/2)^2$.

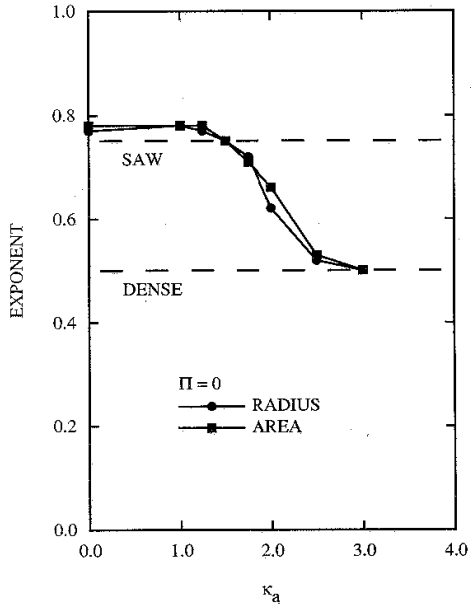

FIG. 3. Characteristic scaling exponents ν and η determined from the vesicle radii of gyration and area. Results are shown for $\Pi=0$ and a range of values for the attraction κ_a. The exponent uncertainty is estimated to be ±0.03.

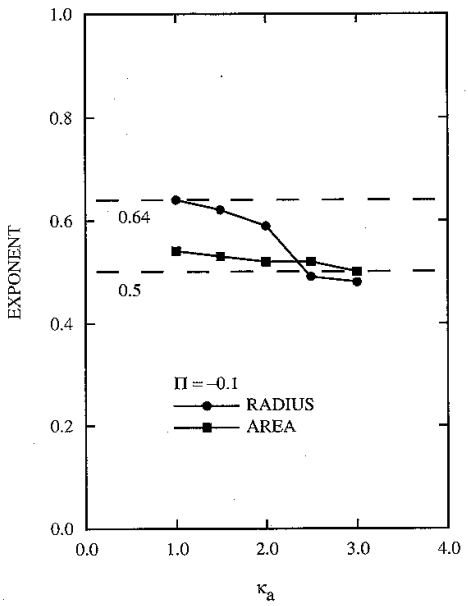

FIG. 4. Characteristic scaling exponents ν and η determined for $\Pi=-0.1$ The area exponent η is $\frac{1}{2}$ in both branched-polymer and dense phases, while ν changes from 0.64 to $\frac{1}{2}$ in these phases, respectively.

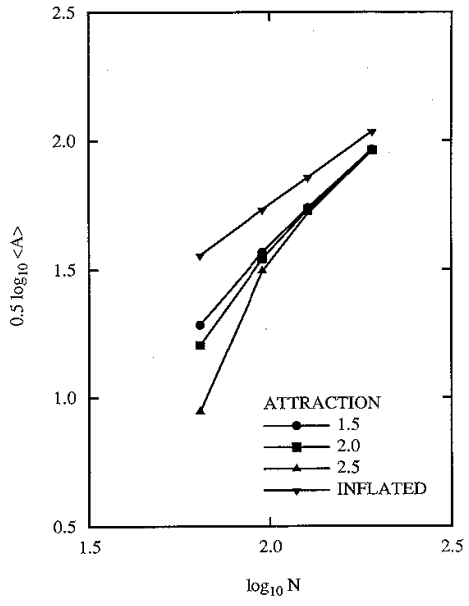

FIG. 5. Logarithmic plot of $\langle A \rangle^{1/2}$, where A is the vesicle area, shown as a function of vesicle size N for pressure $\Pi=0.1$. Three values of the attraction are shown: $\kappa_a=1.5$, 2.0, and 2.5. Areas of the fully inflated vesicles are shown for comparison.

Hence, both the area and energy terms in the enthalpy scale like N. For the small pressures of interest here ($\Pi/\kappa_a \approx 0.05$), the area contribution to the enthalpy can be neglected, and we can write

$$\beta H_{\text{dense}} = -3N\kappa_a \ . \tag{6}$$

The other extreme is the fully inflated configuration in which the perimeter $2Na$ encloses an area of N^2a^2/π. The attraction term is roughly $-\kappa_a N/2^6$, which can be neglected. Hence, we expect

$$\beta H_{\text{inflated}} = -\Pi(N^2/\pi) \ . \tag{7}$$

For a given Π-κ_a combination with $\Pi>0$ and $\kappa_a>2$, we expect the scaling exponents to be equal to $\frac{1}{2}$ at small N in the dense phase and 1 at large N in the inflated phase. As the changeover between these two regimes occurs at intermediate N, the exponents could exceed unity. From Eqs. (6) and (7), the crossover occurs at

$$N = 3\pi\kappa_a/\Pi \ . \tag{8}$$

For example, Eq. (8) predicts a crossover at $N \approx 190$ for $\Pi=0.1$ and $\kappa_a=2$. Although the argument leading up to Eq. (8) is crude, it does indicate that we should see strong finite-size effects in the mass range $64 \le N \le 192$.

The actual behavior of the area at $\Pi=0.1$ is shown in Fig. 5. Several different values of κ_a are shown: 1.5, 2.0, and 2.5. The areas of fully inflated vesicles are shown for comparison. Overall, for the region of N shown, the value of η decreases towards unity as N increases (the fully inflated configurations have $\eta=1$). Also, η moves further from unity as κ_a increases. This behavior is the same as that which leads to Eq. (8). However, we can see that the crossover value for N given by Eq. (8) is too large by at least a factor of 2. This most likely reflects the assumption in Eq. (6) that all beads, including those at the surface of the configuration, have six nearest neighbors. A more accurate determination of the number of nearest neighbors reduces the crossover value closer to what is observed. We conclude that Fig. 5 supports large-N vesicles being inflated at $\Pi>0$.

Having investigated the scaling characteristics of the four vesicle phases, we now turn to their energetics. Typical simulation studies of periodic systems make a finite-size scaling argument to extrapolate to the thermodynamic limit. Our vesicles are finite by their very nature, and the presence of both attraction and the pressure in the enthalpy may make a simple power-law extrapolation to large N difficult.

We begin with the simplest situation, $\Pi=0$, for which $H=E$ in Eq. (2). In the dense region, we expect that the interior beads in configurations such as (b) or (d) in Fig. 2 should have roughly 4–5 nearest neighbors, while the surface beads should have 3–4. Since the rms radii of dense configurations grow like $N^{1/2}$, then the simplest surface corrections to the attractive energy should lead to a scaling form of

$$H/N = a + b/N^{1/2} \tag{9}$$

for the enthalpy per particle. In contrast, the SAW configurations should have an approximately constant value for H/N in the range of N investigated. For $\Pi=0$, we use Eq. (9) as a scaling ansatz to extrapolate to infinite

N. Within our limited data set, we find that Eq. (9) does provide a good description of H/N, the results of the extrapolation being shown in Fig. 6. In the figure, there is a change in the behavior of the enthalpy per particle at κ_a near 2. Although the change appears to be continuous, this could simply reflect poorly determined finite-size effects.

The specific heat as determined by a numerical differentiation of Fig. 6 would yield a smooth curve with a change in slope at around $\kappa_a=2$. To investigate the mass dependence of the specific heat, we use the fluctuation-dissipation expression:

$$C_p/k_B=\frac{1}{N}\beta^2(\langle H^2\rangle-\langle H\rangle^2)\ . \tag{10}$$

For $\Pi=0$, H is equivalent to E. Note that the $2k_BT$ term from particle motion is not generated by Eq. (10) as applied to this simulation. Figure 7 contains the N dependence of C_p as determined from Eq. (10). There appears to be little vesicle mass dependence through the transition region, and C_p appears to be smooth within our resolution. It should be pointed out that in numerical studies[18] of the polymer Θ point, the specific heat as determined by Eq. (10) is shifted at finite N to lower temperatures than the tricritical point. Further, the specific heat cusp observed in such studies is fairly weak, as expected from renormalization-group arguments.[22,23] Our results, as far as they go, are not in disagreement with the polymer studies.[18]

The change from the branched-polymer phase to the dense phase shows the same general features as the SAW to dense transition, as seen by the extrapolated enthalpy per particle for $\Pi=-0.1$ in Fig. 6. Again, the enthalpy does not show strong discontinuities (subject to the usual finite-size caveats). The behavior of the specific heat is also similar to the $\Pi=0$ situation, although our statistics are poorer for $\Pi=-0.1$.

The last observable we wish to discuss is the isothermal compressibility χ_T. Since we have not performed the simulation in small steps in Π, which would allow a determination of χ_T by numerical differentiation of the area expectation $\langle A\rangle$, we use the fluctuation dissipation result

$$\chi_T=\frac{\beta}{\langle A\rangle}(\langle A^2\rangle-\langle A\rangle^2)\ . \tag{11}$$

The results for $\Pi=0$ are shown in Fig. 8 for three different system masses: $N=64$, 128, and 192. The compressibility shows strong finite-size effects in the SAW phase. The change from the SAW phase to the dense phase at around $\kappa_a=2$ is clearly marked by the rapid decrease in the compressibility.

The isothermal compressibility at $\Pi=-0.1$ is shown in Fig. 9, which is plotted with the same scale as Fig. 8 for ease of comparison. The compressibility in the branched-polymer phase is much less than the SAW phase. The compressibility in the dense phase is similar in magnitude to that found at zero pressure.

IV. CONCLUSIONS

We have performed extensive simulations on model vesicles in two dimensions. The vesicles are subject to pressure Π, and have an attractive interaction of strength

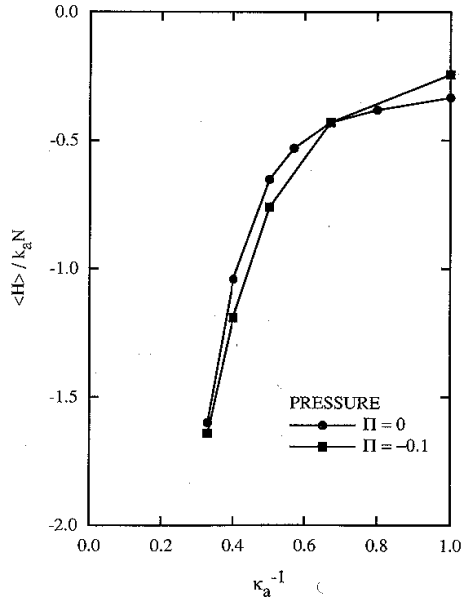

FIG 6. Expectation of the enthalpy per particle $\langle\beta H\rangle/N\kappa_a$ extrapolated to the large N limit by Eq. (9) shown as a function of temperature κ_a^{-1}. Results are shown for both $\Pi=0$ and -0.1.

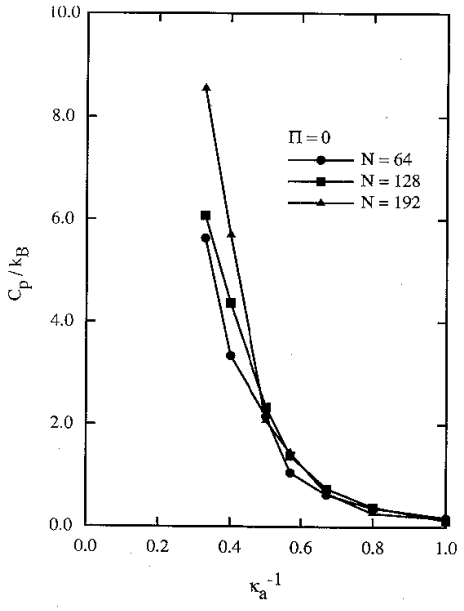

FIG. 7. Specific heat at constant pressure for $\Pi=0$ configurations as extracted from Eq. (10). Three values of the vesicle mass are shown: $N=64$, 128, and 192.

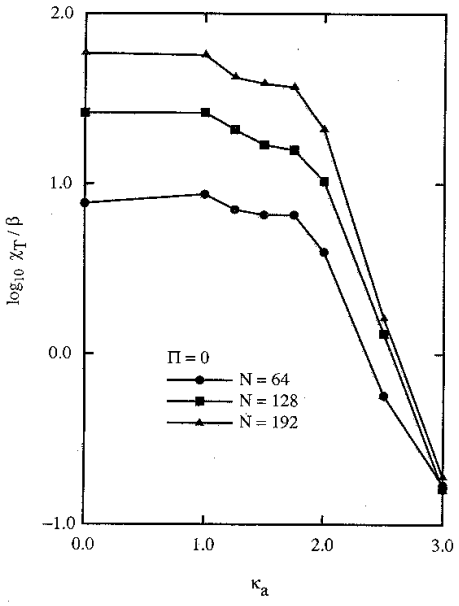

FIG. 8. Isothermal compressibility χ_T/β for $\Pi=0$ as extracted from Eq. (11). Three values of the vesicle mass are shown: $N=64$, 128, and 192.

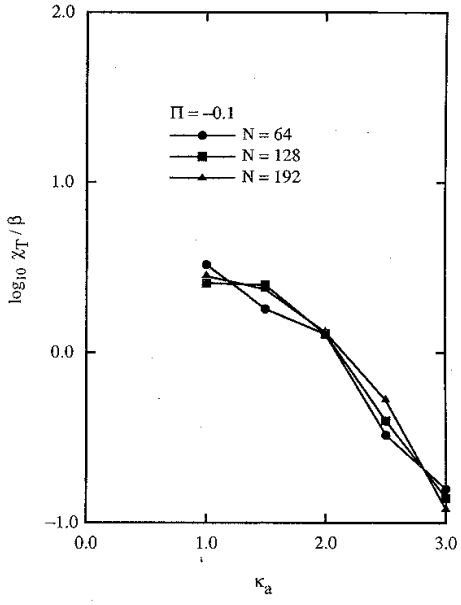

FIG. 9. Isothermal compressibility χ_T/β for $\Pi=-0.1$ as extracted from Eq. (11). Three values of the vesicle mass are shown: $N=64$, 128, and 192.

κ_a between elements on their surface. The vesicle shapes are characterized by their scaling exponents ν and η. At zero pressure, we find that the vesicle shape scales like a self-avoiding walk ($\nu=\eta=\frac{3}{4}$) for $0\leq\kappa_a\leq 2$, but becomes dense ($\nu=\eta=\frac{1}{2}$) for $\kappa_a\geq 2$. For negative pressure $\Pi=-0.1$, the configurations scale like branched polymers ($\nu=0.64$, $\eta=\frac{1}{2}$) for $0\leq\kappa_a\leq 2$, but again become dense for $\kappa_a\geq 2$. At positive pressure, the vesicles are always inflated at large enough N, although there are strong finite-size effects at small N. We explain the approximate magnitude of these finite-size effects as a competition between the attraction and pressure terms in the enthalpy.

The enthalpy per particle shows a change in the same regions of Π-κ_a parameter space as the exponents do, but within our statistics, the changes appear to be smooth. Similarly, the specific heat at constant pressure changes smoothly through the transition region and only begins to rise rapidly at temperatures lower than $\kappa_a^{-1}=\frac{1}{2}$. The isothermal compressibility also changes rapidly with phase, being smallest for the dense phase.

We are unable to determine the order of the transition numerically. The tricritical region ($\Pi=0$, $\kappa_a=2$) is expected[16–23] to have more complicated scaling behavior than the simple forms shown in Eq. (5). We are not able to detect the logarithmic terms in the tricritical region given our range of vesicle sizes. Our specific heat behaves similarly to that observed in numerical studies[18] of the polymer Θ point, in which the maximum of C_p is both weak and shifts to temperatures of the order $\frac{1}{2}$ of the Θ-point temperature for chains with 60 monomers. To investigate the tricritical region will require a much larger range in N than we have examined here.

ACKNOWLEDGMENTS

The author wishes to thank M. Plischke, M. Wortis, and E. Evans for many fruitful discussions. This work is supported in part by the Natural Sciences and Engineering Research Council of Canada.

[1]For a review, see O. G. Mouritsen, in *Molecular Description of Biological Membrane Components by Computer Aided Conformational Analysis,* edited by R. Brasseur (CRC, Boca Raton, FL, 1989).

[2]A. Baumgartner and J. -S. Ho, Phys. Rev. A **41**, 5747 (1990).

[3]S. Leibler and A. C. Maggs (unpublished).

[4]For ground-state studies of 3D systems with axial symmetry, see R. Grebe and M. J. Zuckermann, Biorheology **29**, 735 (1990).

[5]S. Leibler, R. R. P. Singh, and M. E. Fisher, Phys. Rev. Lett. **59**, 1989 (1987); see also M. E. Fisher, Physica D **38**, 112 (1989).

[6]C. J. Camacho and M. E. Fisher, Phys. Rev. Lett. **65**, 9 (1990); A. C. Maggs, S. Leibler, M. E. Fisher, and C. J. Camacho,

Phys. Rev. A **42**, 691 (1990).
[7]B. Duplantier, Phys. Rev. Lett. **64**, 493 (1990).
[8]*Applications of the Monte Carlo Method in Statistical Physics*, edited by K. Binder (Springer-Verlag, Berlin, 1984).
[9]Y. Kantor, M. Kardar, and D. R. Nelson, Phys. Rev. Lett. **57**, 791 (1986); Y. Kantor and D. R. Nelson, *ibid.* **58**, 2774 (1987).
[10]M. Plischke and D. H. Boal, Phys. Rev. A **38**, 4943 (1988); F. F. Abraham, W. E. Rudge, and M. Plischke, Phys. Rev. Lett. **62**, 1757 (1989); D. H. Boal, E. Levinson, D. Liu, and M. Plischke, Phys. Rev. A **40**, 3292 (1989).
[11]D. H. Boal (unpublished).
[12]P. E. Rouse, J. Chem. Phys. **21**, 1272 (1953).
[13]B. Nienhuis, Phys. Rev. Lett. **49**, 1062 (1982).
[14]B. Derrida and D. Stauffer, J. Phys. (Paris) **46**, 1623 (1985).
[15]For reviews of polymer results, see P. -G. de Gennes, *Scaling Concepts in Polymer Physics* (Cornell University, Ithaca, 1979); as well as K. Binder and D. W. Heerman, *Monte Carlo Simulation in Statistical Physics* (Springer-Verlag, Berlin, 1988).
[16]P.-G. de Gennes, J. Phys. (Paris) Lett. **36**, 55 (1975).
[17]For a review of tricritical phenomena, see I. D. Lawrie and S. Sarbach, in *Phase Transitions and Critical Phenomena*, edited by C. Domb and J. L. Lebowitz (Academic, New York, 1984), Vol. 9, p. 1.
[18]K. Kremer, A. Baumgartner, and K. Binder, J. Phys. A **15**, 2879 (1981).
[19]B. Duplantier, Europhys. Lett. **1**, 491 (1986).
[20]F. van Dieren and K. Kremer, Europhys. Lett. **4**, 569 (1987).
[21]E. Eisenriegler and H. W. Diehl, Phys. Rev. B **37**, 5257 (1988).
[22]P.-G. de Gennes, J. Phys. (Paris) Lett. **39**, 299 (1978).
[23]B. Duplantier, J. Phys. (Paris) Lett. **41**, 409 (1980).